



TITLE:

VARIATION OF ELASTICITY IN WATER-SATURATED ROCKS NEAR THE MELTING TEMPERATURE OF ICE

AUTHOR(S):

TAKEUCHI, Shozaburo

CITATION:

TAKEUCHI, Shozaburo. VARIATION OF ELASTICITY IN WATER-SATURATED ROCKS NEAR THE MELTING TEMPERATURE OF ICE. Contributions of the Geophysical Institute, Kyoto University 1972, 12: 157-176

ISSUE DATE:

1972-12

URL:

<http://hdl.handle.net/2433/178611>

RIGHT:

VARIATION OF ELASTICITY IN WATER-SATURATED ROCKS NEAR THE MELTING TEMPERATURE OF ICE

By

Shozaburo TAKEUCHI

(Received August 31, 1972)

Abstract

Compressional and shear wave velocities of water-saturated rhyolite, granite and diabase were measured as a function of temperature near the melting point of ice. Although such porous rocks as the Carleton rhyolite have a large velocity-hysteresis, the hysteresis in low porosity rocks, such as Troy granite, is negligible. Such low porosity rocks are suitable specimens for the simulation of the effects of partial melting. The change of effective bulk modulus of the rocks occurs only in a narrow range of temperature near the melting point of ice, while the change of effective shear modulus occurs gradually over a wider range of temperature. Except for the elastic anomaly, the variation of elasticity in the rocks can be explained by Walsh's equations with an assumed aspect ratio of the inclusions equal to 0.002. While no elastic anomalies are found in polycrystals, the elastic anomaly in water-saturated rocks is found near the melting temperature of ice. The anomaly is attributed to the existence of liquid on the boundary between rock and ice due to local stresses and anomalous melting of ice under pressure.

We predict that an elastic anomaly will exist in any polyphase system near the melting temperature (T_m) of the inclusions whenever $\partial T_m / \partial P < 0$.

We speculate that the origin of the low velocity zone in the upper mantle may be an elastic anomaly of a polyphase system because the melting temperature of some silicate-water system is close to the geotherm and decreases with an increase of pressure.

1. Introduction

A low velocity zone in the upper mantle was detected first by Gutenberg [1948] from the travel times of earthquake-generated body waves. It has been confirmed by many authors (e. g., Gutenberg [1959], Press [1970] and Kanamori [1970]). One suggestion for the origin of the low velocity zone in the upper mantle is partial melting (Press [1959], Takeuchi, *et al.* [1968] and Anderson and Sammis [1970]). The melting point of some rocks is near the temperature of the upper mantle (Shimada [1969] and Wyllie [1971]). The measurement of the velocities of elastic waves in rocks near the melting temperature is therefore important; it is also very difficult experimentally because of the high temperatures and high pressures involved.

To cope with this experimental problem Shimozuru [1954], Mizutani and Kanamori [1964] and Pokorný [1965] measured the elastic wave velocities in Wood's alloy near the melting temperature. In another study Spetzler and Anderson [1969] observed the velocities of the sound in the binary system, NaCl-H₂O. Nur and

Simmons [1969a] studied the effect of viscosity of a fluid phase on the velocity in low porosity rocks.

Here, we report measurements of the seismic wave velocities in low porosity rocks, saturated with water, as a function of temperature near the melting temperature of ice. Timur [1968] has previously reported the velocity of compressional wave only in more porous rocks at permafrost temperatures. However, both the compressional and shear wave velocities are needed for the calculation of the effective bulk and shear moduli. We shall also report on the hysteresis of velocities in rocks with various porosities and discuss the effect of sub-microscopic fractures on the freezing of the ice.

2. Experimental procedures

Cylindrical samples of granite, diabase and rhyolite were prepared from large blocks which had been collected previously. Three of our rocks were used in previous studies and the description of them are given in the references: Chelmsford granite (Birch [1960]), Troy granite (Nur and Simmons [1969b]), Fairfax diabase (Birch [1960] and Simmons [1964]). The elastic properties of Carleton rhyolite have not been measured previously; the petrography was described by Ham, Denison and Merritt [1964]. The cores were one inch in diameter and about two inches long. The ends were ground flat and parallel to within ± 0.001 inches. Physical properties of our specimens are listed in Table 1.

Samples were cleaned up using water and ethyle alcohol and then dried in a vacuum oven at $110^{\circ}C$ for a day. These samples were then moved into an another vacuum chamber to hold at pressure of 10^{-2} torr for another day closing the valve

Table 1. Physical properties of rocks

Specimen		D dry	D wet	P	C	Km	Gm	α
Carleton rhyolite	-I	2.584	2.608	0.024				
	-II	2.550	2.590	0.040				
Troy granite	-I	2.633	2.636	0.003	0.0027	0.572	0.389	0.003
	-II	2.641	2.644	0.003				
	-III	2.640	2.643	0.003				
Chelmsford granite		2.615	2.626	0.010	0.0065	0.566	0.360	0.002
Fairfax diabase		2.950	2.952	0.002	0.0010	0.798	0.425	0.002

D dry=Density of dry rock in *gram/cm³*.
D wet=Density of fully saturated rocks in *gram/cm³*.
P =Total porosity in volume %.
C =Crack porosity in volume %.
Km =Bulk modulus in *Mbar*.
Gm =Shear modulus in *Mbar*.
 α =The aspect ratio

A. See Figure 1 of the block diagram. Then, with the sample still under vacuum, the high vacuum valve A was opened to admit distilled water into the chamber. The sample was left in the water for a day to insure full saturation. This technique is an extension of that reported by Brace *et al.* [1965] and the degree of their saturation was discussed in Brace and Orange [1968].

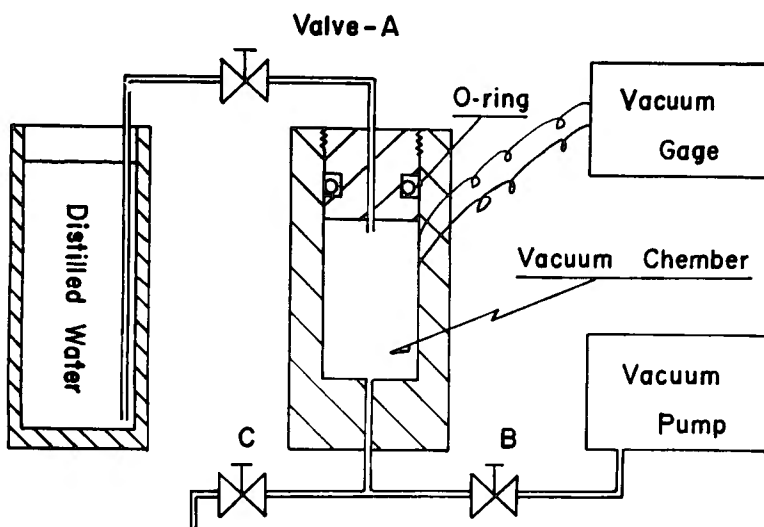


Fig. 1. The block diagram of the water-saturation method. The rock samples were held at pressure of 10^{-2} torr in the vacuum chamber closing the valve A and C for a day. And then the valve B was closed and the high vacuum valve A was opened to admit the distilled water into the chamber.

Ceramic transducers for the study of compressional waves were pasted at each end of the sample with resin (Dow 276-v9) in hot water, clamped tightly and kept in cold water for 12 hours. In the case of shear waves AC cut quartz crystal transducers were epoxied at each end of the sample with Bipax #12 (Tracon Inc.) before the saturation with water. Travel times through the samples were measured by the ultrasonic pulse technique with a mercury delay line similar to that described by Birch [1960] and Simmons [1964]. The time delay of the compressional wave could be consistently reset within ± 0.001 cm Hg for a given specimen at a given temperature with the same amplitude on the oscilloscope display. The time delay of compressional waves in each specimen was 1.2 to 1.6 cm Hg. Thus the precision of measurement of the compressional wave about 0.1% where the accuracy of the velocity was about 1.0%. In the case of the shear wave velocities the precision was also about 0.1% and the accuracy was about 1%.

Velocity measurements were made on the specimen while it was in a refrigerator (Blue M Co.). The surface of the rock cylinder was surrounded by about 7 cm³ of excess water and covered by PVC tubing to contain the water. This assembly was wrapped in fiber glass insulation and placed within the cooling coil of the refrigerator.

tor. The surface temperature of the specimen was measured with an iron-constantan thermocouple to an accuracy of $\pm 0.1^\circ\text{C}$. The surface of the rock was cooled or heated at a constant rate of about $10\text{ min}/^\circ\text{C}$ except at the temperature of 0°C . Before measuring the sound velocity the surface temperature was kept constant for more than ten minutes to allow the temperature inside the rock to approach equilibrium. The distribution of the temperature inside the rock was calculated from the equations given by Carslaw and Jaeger ([1965], p. 199). This calculation is given in Appendix. Near the melting point of the ice the temperature in the refrigerator was kept at -1.0°C while cooling and at $+1.0^\circ\text{C}$ while heating for more than two hours although the 7 cc of water could freeze in less than one hour. The ice surrounding the rock specimen was clear and had no air bubbles. A complete measurement cycle of velocities required about four days.

3. Experimental results

The results with respect to the temperature variation of the compressional wave velocity in Carleton rhyolite are shown in Fig. 2 and of the both compressional and shear wave velocities in Fairfax diabase, Troy granite and Chelmsford granite in Fig. 3. The normalized data, i. e., the points on the smoothed curves, are listed in Table 2. As readily seen from the figures, the velocity in saturated Carleton rhyolite shows a 2.2% hysteresis of the velocity after being cycled through the ice point, while the hysteresis of the velocity in the other rocks is negligible. We infer that the elastic properties of such saturated low porosity rocks as Fairfax diabase, Troy granite and Chelmsford granite may be measured through the ice point without an application of confining pressure. On the other hand, measurements on such rocks as Carleton rhyolite require application of confining pressure to prevent microscopic fractures.

The velocity in the low porosity rocks at a given temperature during cooling is

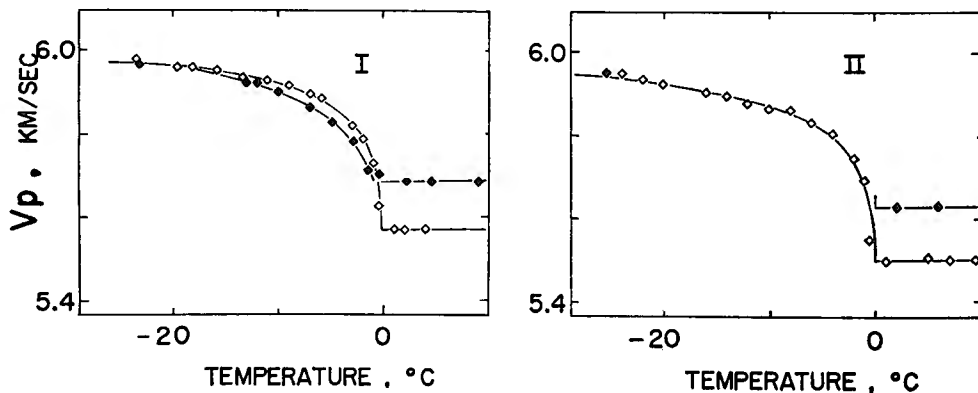


Fig. 2. Compressional wave velocities in water-saturated Carleton rhyolite as a function of temperature. The filled symbols are for the cooling cycles and the white are for heating.

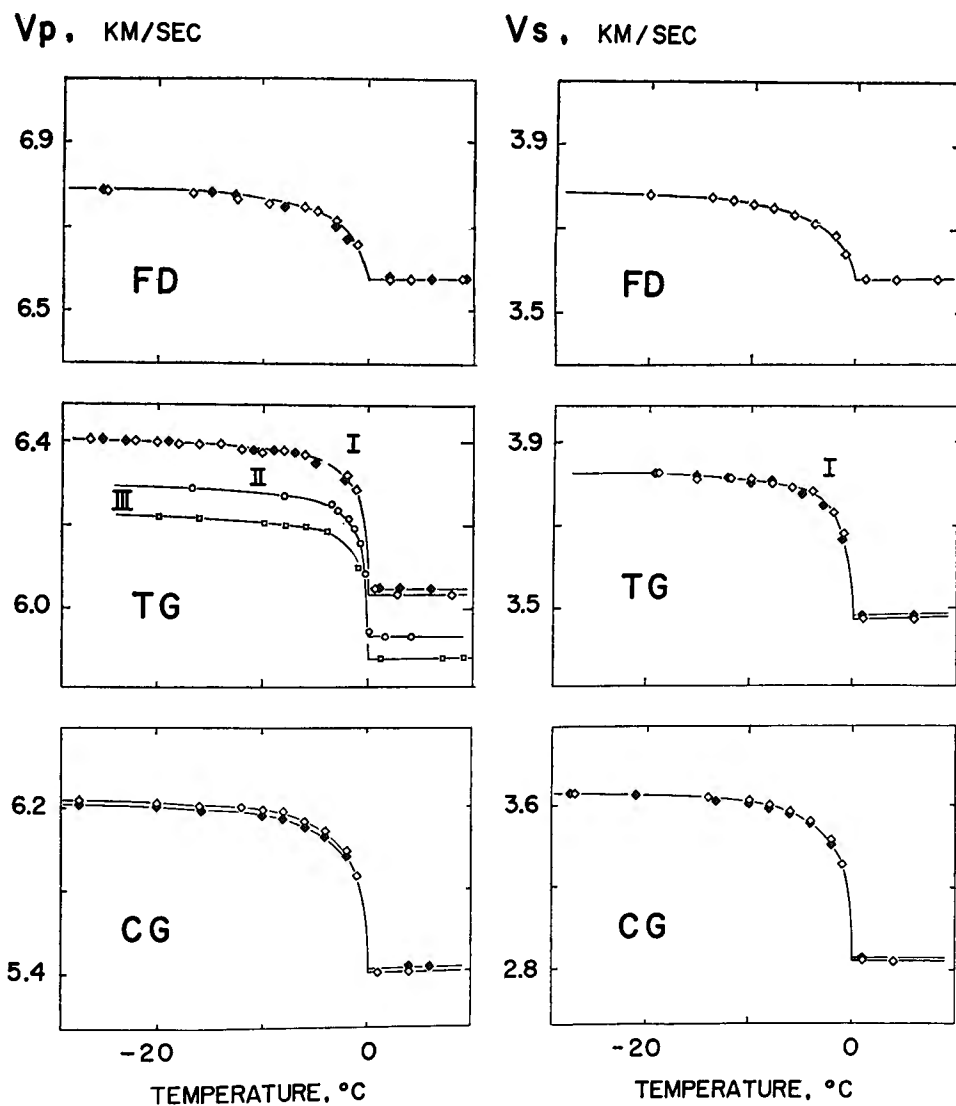


Fig. 3. Compressional and shear wave velocities versus temperature. FD: Fairfax diabase. TG: Troy granite. CG: Chelmsford granite. The Roman numerals on TG are three orthogonal cores. The filled symbols are for the cooling, the white for heating.

the same as that during heating as shown in the Fig. 3. This observation shows that a specimen is near the equilibrium temperature at the time of measurements in both runs. The shape of the velocity versus temperature curves for orthogonal cores of each Troy granite are the same as shown in Fig. 3-TG. This fact can be seen by shifting visually one set of velocity-temperature curves. Each velocity-temperature curves has a point below the ice point where the curve becomes linear with decreas-

ing temperature. The linearity of the velocity-temperature curve was checked to -40°C in the measurement of both velocities in Chelmsford granite.

Table 2. Compressional and shear wave velocities in water-saturated rocks

<i>T</i>	Carleton rhyolite		Troy granite-I		Chelmsford granite		Fairfax diabase	
	<i>V_p</i>	<i>V_p</i>	<i>V_p</i>	<i>V_s</i>	<i>V_p</i>	<i>V_s</i>	<i>V_p</i>	<i>V_s</i>
	(cooling)	(heating)						
-26.0	5.965	5.965	6.410	3.825	6.230	3.649	6.780	3.780
-20.0	5.965	5.965	6.400	3.820	6.218	3.640	6.780	3.780
-16.0	5.945	5.954	6.392	3.815	6.208	3.633	6.780	3.775
-12.0	5.920	5.932	6.384	3.806	6.200	3.625	6.770	3.770
-10.0	5.900	5.920	6.380	3.804	6.190	3.615	6.765	3.762
-8.0	5.878	5.905	6.375	3.800	6.170	3.594	6.755	3.752
-6.0	5.846	5.885	6.370	3.795	6.120	3.560	6.745	3.731
-5.0	5.830	5.818	6.365	3.790	6.100	3.540	6.735	3.729
-4.0	5.810	5.850	6.353	3.780	6.080	3.512	6.725	3.716
-3.0	5.782	5.824	6.335	3.765	6.040	3.475	6.715	3.702
-2.0	5.740	5.785	6.315	3.730	5.980	3.428	6.700	3.685
-1.0	—	5.725	6.280	3.680	5.840	3.310	6.650	3.640
+1.0	5.685	5.565	6.035	3.470	5.383	2.830	6.570	3.581
+4.0	5.685	5.570	6.038	3.470	5.395	2.830	6.575	3.583
+8.0	5.685	5.575	6.042	3.470	5.402	2.830	6.580	3.585

T = Temperature in $^{\circ}\text{C}$.
V_p = Compressional wave velocities in *km/sec*.
V_s = Shear wave velocities in *km/sec*.

4. Discussion

(1) Elasticity of a polycrystal

The first contribution to the elasticity of a polycrystal is given by Voigt [1928] who averaged the elastic stiffnesses over all space. The counterpart of this approach is given by Reuss [1929] who averaged the elastic compliances. Hill [1952] has shown that the Voigt average is a rigorous upper bound and the Reuss average is a rigorous lower bound for the aggregate. The Voigt and Reuss averages are given by:

Voigt

$$K_V = (A + 2B)/3,$$
$$G_V = (A - B + 3C)/5,$$

Reuss

$$K_R = 1/(3a + 6b),$$
$$G_R = 5/(4a - 4b + 3c),$$

$$\left. \vphantom{\begin{matrix} K_V \\ G_V \end{matrix}} \right\} \quad (1)$$

with

$$3A = C_{11} + C_{22} + C_{33}, \quad 3a = S_{11} + S_{22} + S_{33},$$

$$3B = C_{23} + C_{31} + C_{12}, \quad 3b = S_{23} + S_{31} + S_{12},$$

$$3C = C_{44} + C_{55} + C_{66}, \quad 3c = S_{44} + S_{55} + S_{66},$$

C_{ij} = the elastic stiffnesses,

S_{ij} = the elastic compliances.

Hashin and Shtrikman [1962a, b] have derived improved bound by the variational approach. For cubic symmetry the bulk modulus is given unambiguously by

$$K = \frac{1}{3}(C_{11} + 2C_{12}),$$

and the rigidity is bounded by

$$\left. \begin{aligned} G_1^* &= G_1 + 3\left(\frac{5}{G_2 - G_1} - 4\beta_1\right), \\ G_2^* &= G_2 + 2\left(\frac{5}{G_1 - G_2} - 6\beta_2\right), \end{aligned} \right\} \quad (2)$$

where

$$\beta_1 = -\frac{3(K + 2G_1)}{5G_1(3K + 2G_1)},$$

$$\beta_2 = -\frac{3(K + 2G_2)}{5G_2(3K + 4G_2)},$$

$$G_1 = \frac{1}{2}(C_{11} - C_{12}),$$

$$G_2 = C_{44}.$$

The larger of G_1^* and G_2^* is termed the Hashin rigidity, the smaller Shtrikman rigidity by Simmons and Wang [1971] who collected a number of elastic constants of single crystals. They calculated Voigt and Reuss averages for all symmetries but Hashin and Shtrickman bounds for cubic symmetry only. Peselnick and Meister [1965] extended the Hashin and Shtrikman bounds to the case of hexagonal symmetry and trigonal symmetry. In succession, Meister and Peselnick [1966] extended Hashin and Shtrikman bounds to the case of tetragonal symmetry. Hashin and Shtrickman bounds for hexagonal symmetry are given by:

$$K_1^* = K_1 + \frac{K_V - K_1}{1 - \beta_1(C_{11} + C_{12} + C_{13} - 3K_V - 2G_1)},$$

$$\left. \begin{aligned} K_2^* &= K_2 + \frac{K_V - K_2}{1 - \beta_2(C_{11} + C_{12} + C_{33} - 3K_V - 2G_2)}, \\ G_1^* &= G_1 + \frac{B_{21}}{1 + 2\beta_1\beta_{21}}, \\ G_2^* &= G_2 + \frac{B_{22}}{1 + 2\beta_2B_{22}}, \end{aligned} \right\} \quad (3)$$

where

$$K_1 = (C^2 - 6G_1K_V)/(M - 6G_1),$$

$$K_2 = (C^2 - 6G_2K_V)/(M - 6G_2),$$

$$G_1 = \text{Max}(C_{44}, C_{66}),$$

$$G_2 = \text{Min}(C_{44}, C_{66}),$$

$$M = C_{11} + C_{12} + 2C_{33} - 4C_{13},$$

$$C^2 = (C_{11} + C_{12})C_{33} - 2C_{12}^2,$$

$$\begin{aligned} 30B_{21} &= \frac{M - 6G_1}{1 - \beta_1(C_{11} + C_{12} + C_{33} - 3K_1 - 2G_1) - 9\gamma_1(K_V - K_1)} \\ &\quad + \frac{12(C_{66} - G_1)}{1 - 2\beta_1(C_{66} - G_1)} + \frac{(C_{44} - G_1)}{1 - 2\beta_1(C_{44} - G_1)}, \end{aligned}$$

$$\begin{aligned} 30B_{22} &= \frac{M - 6G_2}{1 - 2\beta_2(C_{11} + C_{12} - C_{33} - 3K_2 - 2G_2) - 9\gamma_2(K_V - K_2)} \\ &\quad + \frac{12(C_{66} - G_2)}{1 - 2\beta_2(C_{66} - G_2)} + \frac{12(C_{44} - G_2)}{1 - 2\beta_2(C_{44} - G_2)}, \end{aligned}$$

$$\alpha_1 = -\frac{3}{K_1 + 4G_1} \qquad \alpha_2 = -\frac{3}{3K_2 + 4G_2},$$

$$\beta_1 = -\frac{3(K_1 + 2G_1)}{5G_1(3K_1 + 4G_1)} \qquad \beta_2 = -\frac{3(K_2 + 2G_2)}{5G_2(3K_2 + 4G_2)},$$

$$\gamma_1 = (\alpha_1 - 3\beta_1)/9, \qquad \gamma_2 = (\alpha_2 - 3\beta_2)/9.$$

Kroner [1967] derived the overall elastic moduli of a perfectly disordered polycrystal using the concept of correlation functions. However, the results are shown for cubic symmetry only. Kroner's result is given by:

$$G=G_v\left[1-\frac{12}{125}\frac{\alpha\beta^2}{1-\frac{2}{25}\alpha\beta-\frac{24}{625}\alpha^2\beta^2}\right], \tag{4}$$

where

$$\alpha=\frac{3K+6G_v}{3K+4G_v}, \qquad \beta=\frac{G_2-G_1}{G_v},$$

The single crystal elastic constants of ice (hexagonal symmetry) have been determined by Jona and Scherrer [1952], Green and Mackinnon [1956], Bass *et al.*, [1957], Bogorodskii [1964] and Procter [1966]. Part of these data is listed in Table 3. We calculated the effective mosuli of ice from them with the equations (1) and (3). The results are shown in Table 4. The effective rigidities of ice around the melting temperature have an 8.3% Voigt-Reuss width and a 0.9% Hashin and Shtrikman width. The effective bulk modulus of ice is a narrow band by both methods. Both effective moduli of ice as a function of temerature near the melting point are shown in Fig. 4. Note that the effective moduli of ice versus temperature are almost linear below $-2^{\circ}C$ and a sharp change in the elastic properties occures near the melting point.

Table 3. The elastic stiffnesses (C_{ij}) of ice (hexagonal)

T	D	C_{ij}					REF
		11	12	13	44	55	
0.0	0.9017	.0982	.0633	.0516	.1683	.0336	37
-10.0	0.9017	.1208	.0668	.0713	.1599	.0309	37
-15.0	0.9020	.1337	.0679	.0778	.1302	.0283	37
-2.0	0.9165	.1288	.0609	.0425	.1372	.0300	244
-5.0	0.9168	.1299	.0615	.0431	.1381	.0301	244
-10.0	0.9173	.1315	.0624	.0440	.1395	.0303	244
-15.0	0.9178	.1334	.0635	.0451	.1411	.0305	244
-20.0	0.9183	.1337	.0634	.0454	.1423	.0308	244
-25.0	0.9188	.1338	.0623	.0454	.1430	.0311	244
-16.0	1.064	.1385	.0707	.0581	.1499	.0315	129
-16.0	1.000	.1330	.0630	.0460	.1428	.0326	4
-23.0	0.9200	.1410	.0660	.0624	.1515	.0288	205

T : Temperature in $^{\circ}C$.
 D : Density in gram/cm³.
 C_{ij} : The elastic stiffnesses in *Mbars*.
 REF : (37) Bogorodoskii [1964], (244) Bass, *et al.*, [1957],
 (129) Jona and Scherrer [1952], (4) Green and
 Mackinnen [1956] and (205) Procter [1966].

Table 4. Effective bulk and shear modulus of ice

T	KR	KS	KH	KV	GR	GS	GH	GV	REF
0.0	7.286	7.302	7.307	7.329	2.344	2.438	2.459	2.548	37
-10.0	8.924	9.012	9.020	9.114	3.005	3.027	3.029	3.057	37
-15.0	9.614	9.710	9.712	9.808	3.395	3.403	3.403	3.417	37
-2.0	7.663	7.667	7.667	7.673	3.426	3.476	3.479	3.540	244
-5.0	7.698	7.701	7.702	7.706	3.443	3.492	3.495	3.556	244
-10.0	7.806	7.810	7.810	7.815	3.470	3.520	3.523	3.584	244
-15.0	7.937	7.940	7.940	7.945	3.498	3.549	3.552	3.613	244
-20.0	7.974	7.977	7.977	7.981	3.525	3.575	3.578	3.638	244
-25.0	7.964	7.964	7.964	7.966	3.564	3.613	3.616	3.674	244
-16.0	8.895	8.895	8.895	8.896	3.486	3.517	3.518	3.553	129
-16.0	8.147	8.147	8.147	8.147	3.626	3.653	3.655	3.684	4
-23.0	9.053	9.054	9.055	9.057	3.429	3.474	3.479	3.520	205

K =Effective bulk modulus in 10^{10} dynes/cm².
G =Effective shear modulus in 10^{10} dynes/cm².
V =Averaged according to Voigt's scheme.
S =Shtrikman bound.
H =Hashin bound.
R =Averaged according to Reuss' scheme.
REF=The number of reference for the elastic constants.

The numbers are consistent with the ones in Simmons and Wang (1971).

This observation can be extended to the other polycrystalline aggregates. Elastic constants of KCl, NaCl and AgCl (cubic symmetry) near the melting temperature have been determined by Hunter and Siegel [1942], Stepanov and Eidus [1956], Enck [1960] and the others. The calculated effective moduli, using the equation (4), are shown in Fig. 5. Our inference is also supported by the experimental data on Wood's alloy (Mizutani and Kanamori [1964] and Pokorny [1965]) and NaCl-H₂O solid solutions (Spetzer and Anderson [1968]).

(2) Elasticity of a polyphase system

However, a rock with ice or water filling the interstices is a polyphase system. Aggregation theories of such systems are given by many authors: Hill [1963] has shown the regorous upper bound to a two phase system as follows,

$$\left. \begin{aligned} K &= K_m \left\{ 1 - c \left[\frac{K_m - K_i}{K_m} \right] \right\}, \\ G &= G_m \left\{ 1 - c \left[\frac{G_m - G_i}{G_m} \right] \right\}, \end{aligned} \right\} \quad (5)$$

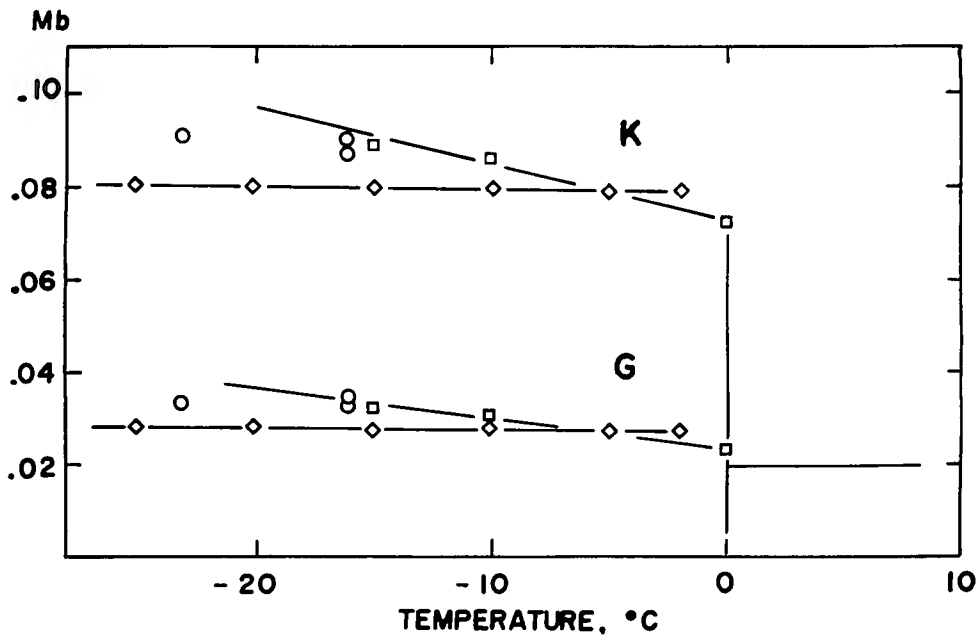


Fig. 4. The bulk and shear moduli of ice versus temperature. The elastic constants of the single crystals are taken from Bogorodoskii [1964] \square and Bass *et al.*, [1957] \diamond and others \circ . The aggregation theories are due to Peselnick and Meister [1965].

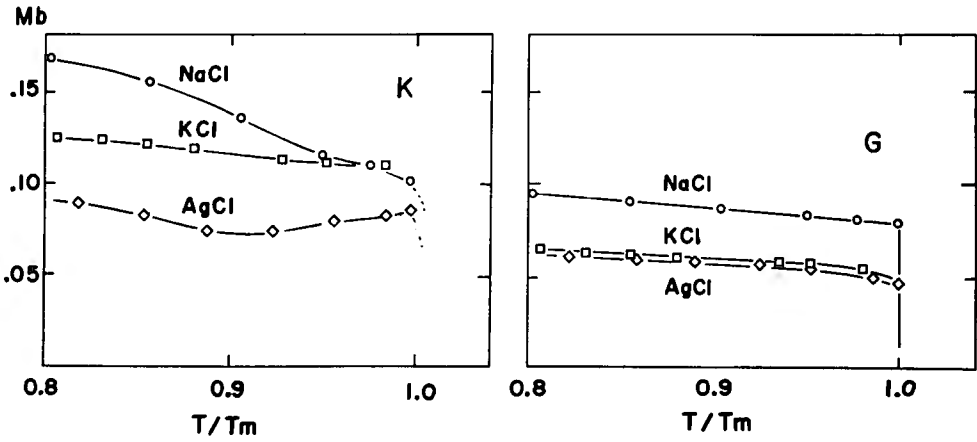


Fig. 5. The bulk and shear moduli of polycrystals versus temperature. The elastic constants of the single crystals are taken from Hunter and Siegel [1942], Stepanov and Eidus [1956] and Enck [1960]. The aggregation theories are due to Kroner [1967].

the lower bounds to it are given as follows;

$$\left. \begin{aligned} K &= K_m \left\{ 1 + c \left[\frac{K_m - K_i}{K_m} \right] \left(\frac{K_m}{K_i} \right) \right\}^{-1}, \\ G &= G_m \left\{ 1 + c \left[\frac{G_m - G_i}{G_m} \right] \left(\frac{G_m}{G_i} \right) \right\}^{-1}, \end{aligned} \right\} \quad (6)$$

where c is the volume concentration of the inclusions. The subscript m denotes matrix and i denotes inclusions. Hashin and Shtrikman [1963] extended Hill's bound to a many phase system. Hashin [1962] has derived the bounds for the elastic moduli of a two or many-phase nonhomogeneous material using the variational approach developed by Hashin and Shtrikman [1962b]. Hashin's bounds are complicated unless the material can be considered to be spherical composite elements.

(3) Elasticity of a dilute suspension

Fortunily we may discuss the rock and ice or water system as a dilute suspension because the ice or water filling the interstices of rocks was always less than 0.01 in the volume ratio (i. e., porosity). The first contribution to the elasticity of a dilute suspension was Einstein's [1906]. From Einstein to Frochlich and Sack [1946], the matrix was assumed to be a Newtonian viscous fluid and the inclusion was spherical. Mackenzie [1952] solved the elasticity of dilute suspension as an elastic problem. In his model a spherical hole was surrounded by a spherical shell of matrix and those in turn were surrounded by a sphere of equivalent homogeneous material. He used a self-consistent method which was developed by Frohlich and Sack [1964]. A more exact calculation for spherical inclusions was given by Sato [1952, 1953]:

$$\left. \begin{aligned} K &= K_m \left\{ 1 - c \left[\frac{K_m - K_i}{K_m} \right] \frac{3K_m + 4G_m}{3K_i + 4G_m} \right\}, \\ G &= G_m \left\{ 1 - c \left[\frac{G_m - G_i}{G_m} \right] \frac{3K_m + 4G_m}{9K_m + 8G_m + 6(K_m + 2G_m)(1 - G_i/G_m)} \right\}, \end{aligned} \right\} \quad (7)$$

Now, assuming the bulk and shear moduli of the inclusions are 0.7990 and 0.4245 Mbars, respectively. See the data of Fairfax diabase of Table 1. When the inclusions are ice and the volume concentration of them is assumed to be 1%, the effective bulk and shear moduli are 0.7800 and 0.42035 Mbars. When the ice melts they become 0.7763 and 0.42035 Mbars. The change of elastic moduli is only 0.47 and 0.00%. Then the effect of phase change of small inclusions is negligible.

A perfect theory for the determination of the elastic field of ellipsoidal inclusions is given by Eshelby [1957]. Wu [1966] has solved the explicit calculation of Eshelby's theory for needle shaped inclusions and for disk shaped inclusions. More generally, Walsh [1969] has given the explicit expression of Eshelby's theory for oblate spheroidal inclusions whose rigidity is much less than the effective rigidity. Walsh's equations are given by:

$$\left. \begin{aligned} K &= K_m \left\{ 1 + c \left[\frac{K_m - K_i}{K_m} \right] \frac{3K_m + 4G_i}{3K_i + 4G_i + 3\pi\alpha G_m (3K_m + G_m)/(3K_m + 4G_m)} \right\}^{-1} \\ G &= G_m \left\{ 1 + c \left[\frac{G_m - G_i}{G_m} \right] \left[0.2 + \frac{1.6G_m}{4G_i + 3\pi\alpha G_m (3K_m + 2G_m)/(3K_m + 4G_m)} \right. \right. \\ &\quad \left. \left. + \frac{0.4(3K_i + 2G_i + 2G_m)}{3K_i + 4G_i + 3\pi\alpha G_m (3K_m + G_m)/(3K_m + 4G_m)} \right] \right\}^{-1} \end{aligned} \right\} \quad (8)$$

where α is the aspect ratio of the inclusions.

(4) Elasticity of water- or ice-saturated rocks

Rocks contain pores and cracks. Pores are spherical shapes and cracks are narrow elliptical shapes. We designate the solid rock and pores as matrix and the ice or water filling the crack spaces as inclusions.

We can calculate the effective bulk and shear moduli from the data of the compressional and shear wave velocities and the densities. In these calculations, the densities of rocks are always taken to be the room temperature values of Table 1. The results are listed in Table 5 and shown in Fig. 6 by the open squares. The bulk and shear moduli of the matrix are unknown but they are assumed to be constant from 10°C to -30°C since the effect of small spherical pores on the elasticity is negligible as previously discussed.

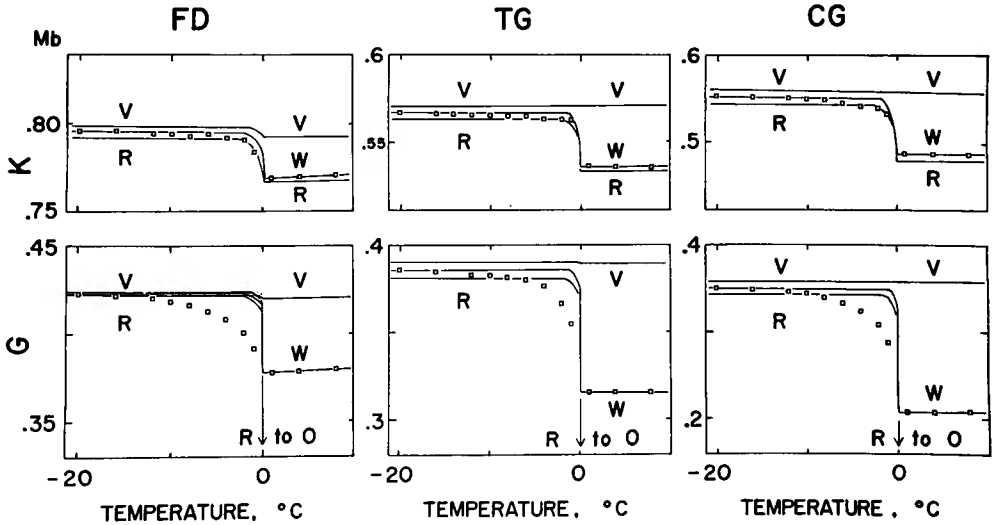


Fig. 6. The bulk and shear moduli of rocks versus temperature. The solid lines are calculated from the methods of V: Voigt, W: Walsh and R: Reuss. The squares are calculated from the measured compressional and shear wave velocities. FD; Fairfax diabase, CG; Chelmsford granite. TG; Troy granite.

We can, therefore, calculate the effective moduli of rock and the porosity and aspect ratio of the inclusions using the equation (8). The fit is made on the computer for Fairfax diabase, Troy granite and Chelmsford granite based on the data in Table 5, except for the shear modulus near the melting point of ice. The results are shown in Fig. 6 by the solid lines marked by W. The assumed aspect ratio of the cracks is about 0.002 in Fairfax diabase and Chelmsford granite and 0.003 in Troy granite, reasonable values. Walsh [1965] concluded that the aspect ratio of low porosity rocks was about 0.002 from his study of the effect of cracks on the compressibility.

Table 5. Effective bulk and shear moduli in water-saturated rocks

<i>T</i>	Troy granite		Chelmsford granite		Fairfax diabase	
	<i>K</i>	<i>G</i>	<i>K</i>	<i>G</i>	<i>K</i>	<i>G</i>
−26.0	0.567	0.385	0.553	0.350	0.795	0.422
−20.0	0.567	0.385	0.551	0.348	0.795	0.422
−16.0	0.566	0.384	0.551	0.347	0.795	0.412
−12.0	0.565	0.382	0.550	0.345	0.794	0.420
−10.0	0.564	0.381	0.549	0.343	0.794	0.418
−8.0	0.564	0.381	0.547	0.399	0.793	0.416
−6.0	0.563	0.380	0.542	0.333	0.795	0.411
−5.0	0.563	0.379	0.540	0.328	0.792	0.411
−4.0	0.562	0.377	0.539	0.324	0.792	0.408
−3.0	0.560	0.374	0.535	0.317	0.792	0.405
−2.0	0.562	0.367	0.528	0.309	0.791	0.401
−1.0	0.563	0.357	0.510	0.288	0.784	0.391
+1.0	0.537	0.317	0.479	0.211	0.770	0.379
+4.0	0.537	0.317	0.483	0.211	0.771	0.379
+8.0	0.537	0.317	0.488	0.211	0.772	0.380

T = Temperature in °C.
K = Effective bulk modulus in Mbar.
G = Effective shear modulus in Mbar.

(5) Elastic anomaly near the melting temperature

The measured effective bulk and shear moduli of rock with ice or water filling the pores agree well with those calculated from Walsh's equations with the exception of the shear modulus near the melting temperature of ice. We attribute this anomaly to the increase of pressure when confined water freezes. Because the melting temperature of ice decreases with pressure (Fig. 7), a layer of water will exist on the boundary between the ice and the rock. Although we cannot calculate explicitly the effect of the liquid on the boundary, we expect a decrease in the effective moduli of rock, especially in shear modulus. At some temperature below the melting temperature of ice no liquid can be found in the rock-ice system under the maximum local stress and then the curves of effective moduli versus temperature become linear. Since

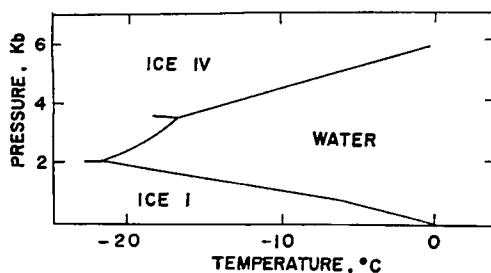


Fig. 7. The melting temperature of H_2O versus pressure, after Bridgman [1937]. The Roman numerals are the phase number.

the minimum temperature of the melting point of ice under high pressure is $-22^\circ C$, no such elastic anomaly will be found at temperatures below $-22^\circ C$. Timur [1968] observed this anomalous behavior of the compressional wave velocity from $0^\circ C$ to $-22^\circ C$ in porous rocks. The lower limit of his elastic anomaly can be explained by the above reason because he applied uniaxial stress on the rock in measuring the velocities.

(6) *Application to the mantle*

Clark and Ringwood [1964] concluded that the partial melt model in the upper mantle is not plausible because observations on the elasticity of NaCl and KCl do not show any anomalies near the melting temperature. Elasticity of polycrystals also shows no anomalies near the melting temperature as discussed previously. However, such discussions should be based on the elasticity of polyphase systems because the mantle is indeed a polyphase aggregate. The fallacy is shown beautifully by the facts that elastic anomaly of rock with ice is found near the melting point of ice although a polycrystal of ice itself has no elastic anomaly.

We may expect a polyphase system to have an elastic anomaly near the melting point of inclusions whose phase diagram is similar to the one of ice as discussed in the last section. Then we may also expect the elastic anomaly in the mantle when it has a phase whose melting temperature is close to the geotherm and decreases with increase of pressure. The melting temperature of some silicate-water systems (for example; albite, Shimada [1969] and gabbro, Wyllie [1971]) is close to the geotherm in the upper mantle and the melting point decreases with an increase of pressure. Thus the origin of the low velocity zone may be an elastic anomaly of a polyphase system near the melting temperature of the inclusions, as Kushiro [1966] and Shimada [1966] have discussed the presence of water in the upper mantle from the existence of low velocity zone.

We did not discuss the effect of viscosity of inclusions to the origins of the low velocity zone as Nur [1971] did. But the viscosity of the liquified phase of them must be even lower than Nur's value. Viscosity of the liquified core is 1 to 10 poises (Miki [1952]). Viscosity of liquid basalt is 10^3 poises at $1200^\circ C$ while the viscosity

of solid basalt is higher than 10^{12} poises at 800°C (Takeuchi, [1969]). The effect of pressure on viscosity is small and the presence of water decreases the viscosity (Murase [1965]). The effect of viscosity on velocity is negligible when the viscosity of the inclusions in polyphase system is low. Then the origin of the low velocity zone is not due to the effect of the viscosity of them.

5. Conclusions

(1). Low porosity rocks with ice filling the pores are suitable elastic analogues to study velocities in polyphase systems near the melting point of one phase because the velocity hysteresis is negligible. (2). The change of effective bulk modulus of such rocks occurs over a narrow range of temperature near the melting point of ice. The change of effective shear modulus occurs gradually over a wider range of temperature. (3). Except near the melting point of ice, the variation of elasticity of the rocks can be explained by Walsh's equations with the aspect ratio of the inclusions at 0.002. (4). While a number of polycrystals including ice has no elastic anomaly near the melting temperature, an elastic anomaly, especially in the shear modulus, is found in water-saturated rocks near the melting point of ice. (5). The anomaly likely results from the existence of liquid on the boundary of rock and ice due to local stresses and the anomalous melting of ice under pressure. (6). We predict that such elastic anomaly exists for any polyphase system near the melting temperature of inclusions provided that the melting point decreases with an increase of pressure. (7). The low velocity zone in the upper mantle is due to an elastic anomaly of a polyphase system since the melting temperature of some silicates with water is close to the geotherm and decreases with increase of pressure.

Appendix

Assuming that the temperature inside a rock was a function of radius and time, the equation of thermal conduction in the rock is

$$\frac{\partial u}{\partial t} = k \left(\frac{\partial^2 u}{\partial r^2} + \frac{1}{r} \frac{\partial u}{\partial r} \right), \quad (\text{A1})$$

where u = the temperature $^{\circ}\text{C}$,

r = the radial coordinate in cm ,

t = the time in seconds,

k = the thermal diffusivity in a rock in $\text{cm}^2/\text{degree}$.

When the surface temperature of the rock changes as a step function of time, the initial and boundary condition become

$$\left. \begin{aligned} u &= 0 \text{ at } t=0 \text{ in } 0 \leq r \leq a, \\ u &= u_0 \text{ at } t > 0 \text{ in } r = a, \end{aligned} \right\} \quad (\text{A2})$$

where a = radius of the rock,

u_0 = a constant temperature.

The solution of equation (A1) with the initial and boundary conditions (A2) is given by:

$$u = u_0 \left\{ 1 - \frac{2}{a} \sum_{n=1}^{\infty} e^{-\kappa \alpha_n^2 t} \frac{J_0(r \alpha_n)}{\alpha_n J_1(a \alpha_n)} \right\}, \quad (\text{A3})$$

where $\alpha_n = 1, 2, 3, \dots$ are the roots of $J_0(\alpha_n) = 0$.

When the density of the rock is 2.60 gram/cm^3 , the heat capacity is $0.21 \text{ cal/gram degree}$ and the thermal conductivity is $0.008 \text{ cal/cm sec degree}$, then the thermal diffusivity k of the rock becomes $0.015 \text{ cm}^2/\text{sec}$. The temperature distribution at various times t inside the rock whose radius is 1.27 cm (0.5 inches) was calculated and the temperature at the center of the rock at various times is given in Fig. (A-left).

When the temperature on the surface of the rock is given by $\phi = ct$ where c is a constant, the initial and the boundary conditions become:

$$\left. \begin{aligned} u &= 0 \text{ at } t=0 \text{ in } 0 \leq r < a, \\ u &= ct \text{ at } t > 0 \text{ in } r = a, \end{aligned} \right\} \quad (\text{A4})$$

where a is the radius of the rocks.

Solution of equation (A1) with the initial and the boundary conditions (A4) is given by;

$$u = c \left(t - \frac{a^2 - r^2}{k} \right) + \frac{2c}{ak} \sum_{n=1}^{\infty} e^{-k \alpha_n^2 t} \frac{J_0(r \alpha_n)}{\alpha_n^3 J_1(a \alpha_n)}, \quad (\text{A5})$$

The difference of the temperature between the center of the rock and the surface of the rock is:

$$\Delta u = \frac{ca^2}{4k} - \frac{2c}{ak} \sum_{n=1}^{\infty} \frac{e^{-k \alpha_n^2 t}}{\alpha_n^3 J_0(a \alpha_n)}, \quad (\text{A6})$$

when the temperature at the surface of the rock is 1°C , the difference of the temperature between the center and the surface as a function of the rate of cooling (or heating) is given in Fig. (A-right).

From these calculations we conclude that we should keep a constant surface temperature for two minutes after a change of 1 degree to insure a uniform internal tem-

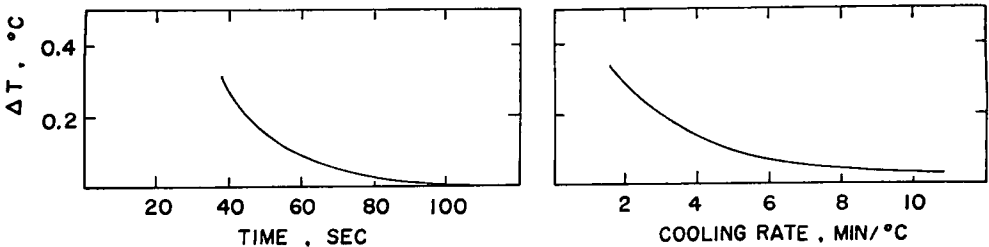


Fig. (A) The difference of temperature between the center of a rock and the surface of it as a function of time in second (left) and of the cooling rate in minutes per $^\circ\text{C}$ (right).

perature before measuring the velocity of sound in the rock. Or we could maintain an equilibrium temperature in the rock by changing the surface temperature at the rate of one degree per ten minutes.

Acknowledgements

I am indebted to Professor Gene Simmons of Massachusetts Institute of Technology (MIT) who encouraged me throughout the whole work. My thanks are due to Dr. Herbert Wang, Mr. Terry Todd and Mrs. Ruth Fitterman of MIT for much help. This work was almost done while I was at Earth and Planetary Sciences of MIT. I also thank Professors Haruo Miki and Izuo Ozawa of Kyoto University who recommended me for study at MIT. I wish to thank Mr. Toratoro Takeuchi Certified Public Accountant who gave me the travel grant to MIT and back. Further financial support was provided by the National Science Foundation, grant number *NGR 22-009-540*.

References

- Anderson, D. L. and C. Sammis, 1970; Partial melting in the upper mantle, *Phys. Earth Planet. Int.*, **3**, 43–50.
- Bass, R., D. Rossberg and G. Ziegler, 1957; Die elastischen Konstanten des Eises, *Zeit. Phys. Ed.*, **149**, 199–203.
- Birch, F., 1960; The velocity of compressional waves in rocks to 10 kilobars, Part 1, *J. Geophys. Res.*, **65**, 1083–1120.
- Bogorodskii, V. V., 1964; Elastic moduli of ice crystals, *Soviet Phys. Acous.*, **10**, 124–126.
- Brace, W. F., A. S. Orange and T. R. Madden, 1965; The effect of pressure on the electrical resistivity of water-saturated crystalline rocks, *J. Geophys. Res.*, **70**, 5669–5678.
- Brace, W. F. and A. S. Orange, 1968; Further studies of the effects of pressure on electrical resistivity of rocks, *J. Geophys. Res.*, **73**, 5407–5420.
- Bridgman, P. W., 1911; Water, in the liquid and five solid forms, under pressure; *Daedalus*, *Proc. Amer. Acad.*, **47**, 441–558.
- Carlsaw, H. S. and J. C. Jaeger, 1959; *Conduction of Heat in Solid*, second edition, Oxford University Press,
- Clark, S. P., Jr. and A. E. Ringwood, 1964; Density distribution and constitution of the mantle, *Rev. Geophys.*, **2**, 35–88.
- Einstein, A., 1906; Eine neue Bestimmung der Molekuldimensionen, *Ann. Phys.*, **19**, 289.
- Enck, F. D., 1960; Behavior of the principal elastic moduli and specific heat at constant volume of KCl at elevated temperatures, *Phys. Rev.*, **119**, 1873–1877.
- Eshelby, J. D., 1957; The determination of the elastic field of an ellipsoidal inclusion and related problems, *Proc. Roy. Soc., London*, (A) **241**, 376–396.
- Frohlich, H. and R. Sack, 1946; Theory of the rheological properties of dispersions, *Proc. Roy. Soc., London*, (A) **185**, 415.
- Green, R. E., Jr. and Mackinnon, 1948; Determination of the elastic constants of ice single crystals by an ultrasonic pulse method, *J. Acous. Soc. Amer.*, **28**, 1292.
- Gutenberg, B., 1948; On the layer of relatively low velocity at a depth of about 80 kilometers, *Bull. Seis. Soc. Amer.*, **38**, 121.
- Gutenberg, B., 1959; *Physics of the Earth's Interior*, Academic Press, New York and London, 140 pp.

- Ham, W. E., R. E. Denison and C. A. Merritt, 1964; Basement rocks and structural evolution of southern Oklahoma, Oklahoma Geol. Survey Bull., **95**, 38.
- Hashin, Z., 1962; The elastic moduli of heterogeneous materials, J. Appl. Mech., **29**, 143.
- Hashin, Z. and S. Shtrikman, 1962a; On some variational principles in anisotropic and nonhomogeneous elasticity, J. Mech. Phys. Solids, **10**, 335-342.
- Hashin, Z. and S. Shtrikman, 1962b; A variational approach to the theory of the elastic behaviour of polycrystals, J. Mech. Phys. Solids, **10**, 343-352.
- Hill, R., 1952; The elastic behaviour of a crystalline aggregate, Proc. Phys. Soc., London (A) **65**, 349.
- Hill, R., 1963; Elastic properties of reinforced solid: some theoretical principles, J. Mech. Phys. Solids, **11**, 357-372.
- Hunter, L. and S. Siegel, 1942; The variation with temperature of the principal elastic moduli of NaCl near the melting point, Phys. Rev., **58**, 84-90.
- Jona, F. and P. Scherrer, 1970; Die elastischen Konstanten von Eis Einkristallen, Helv. Phys. Acta, **25**, 35-54.
- Kanamori, H., 1970; Velocity and Q of mantle waves, Phys. Earth Planet. Int., **2**, 259-275.
- Kroner, E., 1962; Elastic moduli of perfectly disordered composite materials, J. Mech. Phys. Solids, **15**, 319-329.
- Kushiro, I., 1966; State of H₂O in the mantle, Bull. Volc. Soc. Japan, **11**, 116-126.
- Mackenzie, L. K., 1950; The elastic constants of a solid containing spherical holes, Proc. Roy. Soc. London, (B) **63**, 2-11.
- Meister, R. and L. Peshnick, 1966; Variational method of determining effective moduli of polycrystals with tetragonal symmetry, J. Appl. Phys., **37**, 4121-4125.
- Miki, H., 1952; Physical states of the Earth's core, J. Phys. Earth, **1**, 67-74.
- Mizutani, H. and H. Kanamori, 1964; Variation of elastic wave velocity and attenuative property near the melting temperature, J. Phys. Earth, **12**, 43-49.
- Murase, T., 1965; Magma and physical properties of volcanic rocks, Bull. Volc. Soc. Japan, **10**, 153-158.
- Nur, A., 1971; Viscous phase in rocks and the low-velocity zone, J. Geophys. Res., **76**, 1270-1277.
- Nur, A. and G. Simmons, 1969a; The effect of viscosity of a fluid phase on velocity in low porosity rocks, Earth, Plan. Sci. Lett., **7**, 99-108.
- Nur, A. and G. Simmons, 1969b; The effect of saturation on velocity in low porosity rocks, Earth Plan. Sci. Lett., **7**, 183-193.
- Peselnick, L., and R. Meister, 1965; Variational method of determining effective moduli of polycrystals: (A) hexagonal symmetry (B) trigonal symmetry, J. Appl. Phys., **36**, 2879-2884.
- Pocorny, M., 1965; Variation of velocity and attenuation of longitudinal waves during the solid liquid transition in Wood's alloy, Studia Geophys. Geodaet. Českoslov. Acad. V'ed., **9**, 250.
- Press, F., 1959; Some implications on mantle and crustal structure from G wave and love waves, J. Geophys. Res., **64**, 565-568.
- Press, F., 1970; Earth models consistent with geophysical data, Phys. Earth Planet. Int., **3**, 3-22.
- Proctor, T. M., 1966; Low-temperature speed of sound in singlecrystal ice, Acoust. Soc. Amer. J., **39**, 972-977.
- Reuss, A., 1929; Berechnung der Fließgrenze von Mischkristallen auf Grund der Plastizitätsbedingung für Einkristalle, Z. Angew. Math., **9**, 49.
- Sato, Y., 1952; Velocity of elastic waves propagated in media with small holes, Bull. Earthq. Res. Inst., Tokyo Univ., **30**, 179-190.
- Sato, Y., 1953; Velocity of elastic waves propagated in media with small obstacles, Bull. Earthq. Res. Inst., Tokyo Univ., **31**, 1-18.
- Shimada, M., 1966; Effects of pressure and water on the melting of basalt, Spec. Contr. Geophys. Inst., Kyoto Univ., **6**, 303-311.

- Shimada, M., 1969; Melting of albite at high pressures in the presence of water, *Earth Planet. Sci. Let.*, **6**, 447–450.
- Shimozuru, D., 1954; Study on the elasticity near the melting point. Part I, Nature of dilatational wave, *Bull. Earthq. Inst., Tokyo Univ.*, **32**, 271–279.
- Simmons, G., 1964; Velocity of shear waves in rocks to 10 kilobars, 1, *J. Geophys. Res.*, **69**, 1123–1130.
- Simmons, G. and H. Wang, 1971; *Single Crystal Elastic Constants and Calculated Aggregate Properties: A Handbook*, second edition, The M. I. T. Press, Cambridge, Mass., 370 pp.
- Spetzler, H. and D. L. Anderson, 1968; The effect of temperature and partial melting on velocity and attenuation in a simple binary system, *J. Geophys. Res.*, **73**, 6051–6060.
- Stepanov, A. V. and I. M. Eidus, 1956; Temperature dependence of the elastic constants of monocrystals of sodium chloride and silver chloride, *Soviet Phys. JETP*, **2**, 377–382.
- Takeuchi, S., 1969; Viscosity and yielding of basalt under high temperature, *J. Phys. Earth*, **17**, 91–94.
- Takeuchi, H., Y. Hamano and Y. Hasegawa, 1968; Raylei- and Love- wave discrepancy and the existence of magma pocket, *J. Geophys. Res.*, **73**, 3349–3350.
- Timur, A., 1968; Velocity of compressional waves in porous media at permafrost temperatures, *Geophysica*, **33**, 584–595.
- Voigt, W., 1928; *Lehrbuch der Kristallphysik*, B. G. Teubner, Leipzig.
- Walsh, J. B., 1965; The effect of cracks on the compressibility of rock, *J. Geophys. Res.*, **70**, 381–389.
- Walsh, J. B., 1969; New analysis of attenuation in partially melted rock, *J. Geophys. Res.*, **74**, 4333–4337.
- Wu, T. T., 1966; The effect of inclusion shape on the elastic moduli of a two-phase material, *Int. J. Solids Structures*, **2**, 1–8.
- Wyllie, P. J., 1971; Role of water in magma generation and initiation of diapiric uprise in the mantle, *J. Geophys. Res.*, **76**, 1328–1338.